

OPEN ACCESS
Full open access to this and thousands of other papers at <http://www.la-press.com>.

Identification of a Gene Expression Signature Common to Distinct Cancer Pathways

Niklaus Fankhauser¹, Igor Cima^{1,2}, Peter Wild^{1,3} and Wilhelm Krek¹

¹Institute of Molecular Health Sciences, ETH Zurich, CH-8093 Zurich, Switzerland. ²Institute of Bioengineering and Nanotechnology, A*STAR, Singapore 138669, Singapore. ³Institute of Surgical Pathology, Department Pathology, University Hospital Zurich, CH-8091, Zurich, Switzerland.

Corresponding author email: wilhelm.krek@cell.biol.ethz.ch

Abstract: Mutations in cancer-causing genes induce changes in gene expression programs critical for malignant cell transformation. Publicly available gene expression profiles produced by modulating the expression of distinct cancer genes may therefore represent a rich resource for the identification of gene signatures common to seemingly unrelated cancer genes. We combined automatic retrieval with manual validation to obtain a data set of high-quality gene microarray profiles. This data set was used to create logical models of the signaling events underlying the observed expression changes produced by various cancer genes and allowed to uncover unknown and verifiable interactions. Data clustering revealed novel sets of gene expression profiles commonly regulated by distinct cancer genes. Our method allows retrieval of significant new information and testable hypotheses from a pool of deposited cancer gene expression experiments that are otherwise not apparent or appear insignificant from single measurements. The complete results are available through a web-application at <http://biodata.ethz.ch/cgi-bin/geologic>.

Keywords: cancer genes, gene microarray database analysis, gene expression signatures, meta-analysis, network interactions, clustering

Cancer Informatics 2012:11 139–146

doi: [10.4137/CIN.S9542](https://doi.org/10.4137/CIN.S9542)

This article is available from <http://www.la-press.com>.

© the author(s), publisher and licensee Libertas Academica Ltd.

This is an open access article. Unrestricted non-commercial use is permitted provided the original work is properly cited.

Introduction

The development of cancer requires multiple genetic alterations perturbing distinct cellular pathways. In human cancers, these alterations often arise owing to mutations in tumor suppressor genes and proto-oncogenes, which in turn trigger uncontrolled cell proliferation, survival and genomic instability. Consequently, the study of tumor suppressor proteins and proto-oncogenes and the cellular signaling networks deregulated by the corresponding mutant proteins has become a centerpiece of contemporary cancer research. In fact, investigations of their mode of action have pinpointed key mechanisms that protect humans against tumor development and thus provided rational foundations for preventing, detecting, and treating cancer.

Inactivation of tumor suppressor genes or the activation of oncogenes invariably trigger changes in gene expression programs. DNA microarrays¹ are in wide use as a method to quantify changes in global expression levels. Public microarray databases contain measurements of transcription programs in cells under thousands of different biological conditions and/or perturbations. One of the most prominent is NCBI Gene Expression Omnibus (GEO),² a curated repository containing microarray data in a standardized format.³ This database therefore offers a rich resource of quantitative data on the behavior of gene expression changes in response to cancer gene mutations.

By specifically analyzing gene expression program changes associated with cancer gene activation or inactivation, we sought for signatures shared among distinct cancer genes listed in the census of cancer genes⁴ and integrated the resultant data sets into logical networks of interactions.

Meta-analysis of cancer microarray data has been successfully applied by Rhodes et al to find a common gene-expression signature⁵ in independent data sets from different cancer types. Ramaswamy and colleagues discovered a predictive signature⁶ for the metastatic status of tumors from diverse origins and Creighton reported coordinate expression patterns of multiple oncogenic pathway signatures⁷ in human prostate tumors. Our approach used measurements from cell culture experiments in which the expression of specific cancer-causing genes has been either induced or downregulated. This allowed us to unveil

gene expression signatures common to cancer genes that have not been linked previously.

Methods

Selection and acquisition

As outlined in Figure 1, the first step in data acquisition was searching the 385 genes present in the cancer

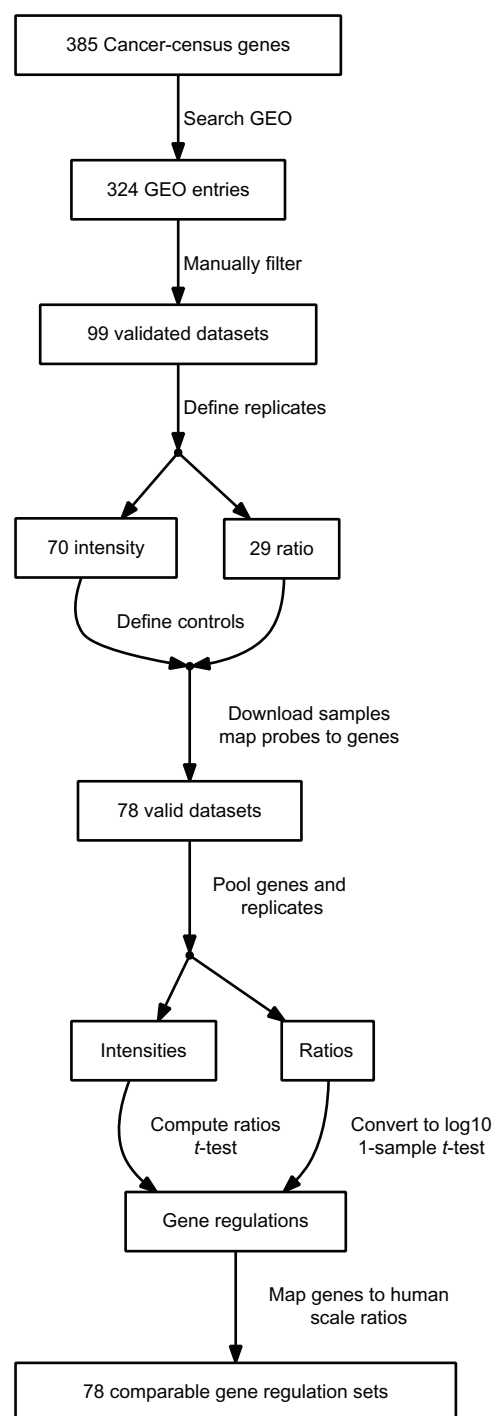


Figure 1. Flowchart of the data acquisition process.



gene census in the NCBI GEO repository. 324 GEO entries contained one of these gene names in the title or abstract. The descriptive fields of the entries were duplicated into a local database. False positives were made apparent through an appropriate visualization of the entry description and subsequently removed. We selected experiments in which cancer genes were over-expressed, depleted by the application of small interfering RNAs or genetically eliminated by virtue of gene knock-out in mice. In addition, we included experiments in which dominant-negative forms of cancer genes were expressed. All of these 99 experiments were performed in either human, mouse or rat cell lines as described in the publication accompanying the experiment. If the measured values were given as raw intensities, samples for induced and control as well as their replicates were selected. Replicates and type of logarithm were selected for entries providing ratios. The definition database was made accessible from network-edges in the web-interface.

Expression values were retrieved for the 607 defined samples. The probe identifiers were mapped to Entrez gene identifiers using the microarray platform description provided by GEO and the UniGene database.⁸ 78 data sets were successfully mapped, the remaining 21 did not contain valid identifiers. NCBI HomoloGene provided human homologues of mouse and rat genes. Measurements were available for 18885 genes, while there was a total of 19978 human genes in HomoloGene. The probe-level measurements ($N = 9981226$) were grouped by genes and replicates. Intensity values were grouped into induced/control to compute the $\log(\text{ratio})$ as well as the P -value of a t -test. In the case of entries containing ratios, they were converted to base 10 logarithm and a one-sample t -test was performed. In order to be able to filter sets of comparably regulated genes, the \log -ratios were scaled by subtracting the experiment mean and dividing by the standard deviation. These computations were performed using the Python programming language. The final data matrix is available for download from <http://biodata.ethz.ch/cgi-bin/geologic> at the bottom of the page.

Clustering

Automatic classification and multiscale bootstrap resampling was performed using the R⁹ package *pvclust*.¹⁰ A matrix consisting of experiments as

columns, genes as rows and gene-expression changes for each pair was used as input. Because not every gene was present in all of the microarray experiments, there are missing values in this matrix. An iterative method was used to reduce the fraction of missing values. In each step, the row or column containing the largest fraction of missing values was removed from the matrix. This procedure was repeated until no more rows or columns contained a fraction of missing values larger than the desired threshold.

The matrices ranging from 1% to 33% missing value thresholds (termed “namax” in the web-application) were computed. Each of them was separately clustered and the resulting dendrograms were made available through the web-application. Negative correlation distance of pairwise complete observation was used as the distance measure. The average linkage method was used in hierarchical clustering. The relative size of the bootstrap sample was increased from 50% to 140% in 10 steps. At each step, 1000 bootstrap replications were performed.

Interaction network analysis

In order to find the significant gene expression changes in our data sets, thresholds were set on the P -value as well as the magnitude of the change between induced and control. As previously described, each microarray data set originates from an experiment in which the expression of a gene has been altered by genetic methods. Therefore, a set of 56 “altered genes” is defined. If in any of the data sets one of the other “altered genes” is significantly changed, a connection between this and the one altered in the data set is created. The collectivity of these connections define a network (directed graph) which was plotted using the Graphviz graph visualization software¹¹ and displayed as Scalable Vector Graphics (SVG) or in the ZGRViewer Java applet.¹² The P -value and expression change threshold was made variable in the web-application. A default threshold of P -value below 0.01 and $\text{abs}[\log_{10}(\text{ratio})]$ above 1.5 provided an appropriate number of interactions. The network was searched for sub-networks, in which the direction of gene expression change matched the perturbation in an experiment studying this gene.

The novelty of the gene interactions was determined by searching PubMed. Edges in the web-application link to the manually confirmed PubMed source



sentences. The web-application can be controlled through a menu at the top, where the first item (“HELP”) provides information on usage.

Transcription factor analysis

The TRANSFAC database of transcription factors and their binding sites¹³ was acquired from BIOBASE. All human genes annotated with known binding sites were extracted from the “GENE” table. The gene-factor pairs found by in-vivo ChIP-chip and ChIP-Seq experiments were extracted from the “FRAGMENT” table. Promoter sequences of all human genes from -5000 to +500 relative to the transcriptions start site were retrieved from the ENSEMBL database (version GRCh37) using the Perl API. The “match” program provided by BIOBASE was used to detect further binding sites in these sequences, using the non-redundant vertebrate profile, where matrices from the “MATRIX” table were selected with respect to minimize the rate of false positives. Matches exhibiting a matrix similarity scores above 0.9 were used. Finally, these three data-sets were pooled into one table containing 1458399 gene to binding-site pairs. Over-representation of transcription factor targets in gene sets was detected by a Fisher exact test.

Results and Discussion

Clustered experiment groups

Searching for microarray measurements based on the reported census of genes causally linked to cancer progression⁴ resulted in 78 individual studies, performed on 56 cancer genes. Table 1 shows which cancer genes were present in which type of perturbation. The processed data matrix of these 78 experiments

Table 1. Cancer genes.

Increased	Decreased
AKT1, BCL2, BRAF, EBF1, EGFR, ERBB2, ERG, FGFR2, FGFR3, GATA6, HOXC13, HRAS, KIT, KRAS, MAP2K1, MKL1, NOTCH1, PPARG, RAF1, RB1, RET, WT1	APC, ATM, BCL11A, BCL11B, BRCA1, CARD11, CDX2, CREB1, FH, FUS, HNF1A, HOXA11, HOXA9, IRF4, JAK2, MET, MYC, NF1, NOTCH1, NRAS, PARP1, PAX5, PBX1, POU5F1, PPARG, PTEN, RAG1, RBM15, RELA, RING1, RUNX1, SDHB, TFRC, TP53, VHL, WRN, WT1

with expression levels for an average of 12517 genes contained 34% missing values. In order to find groups of experiments in which genes are similarly regulated, this data matrix was clustered. Groups of cancer genes along known classical pathways were detected with high significance in bootstrapped clustering, corroborating the methodology. The dendrograms in the web-application shows clusters above the 95% significance level highlighted by red rectangles. The numbers in red next to the dendrogram branches are the “Approximately Unbiased” (AU) values provided by pvclust, from which the *P*-value can be deduced by $1 - AU/100$.

The largest group of genes repeatedly detected in clustering analysis (*P*-value = 0.05) were based on the following experiments and brought about by cancer genes previously not known to induce common gene expression changes. These include murine sarcoma viral oncogene homolog B1 (BRAF) elevated (+), breast cancer 1 (BRCA1) reduced/absent (-), Notch homolog 1 (NOTCH1) (-), homeobox A9 (HOXA9) (-) and erythroblastosis virus E26 oncogene homolog (ERG) (+). As these perturbations lead to a common gene expression signature, it can be hypothesized that the signaling pathways that these distinct cancer genes affect converge to change a common program in gene expression. Therefore, it is conceivable that deregulated expression of this set of genes contributes to one or more general aspects of the cancer phenotype. Complete results are available in the web-application through the “Experiment Clusters” link.

In-depth analysis

The most significant cancer gene group that produced a common gene expression signature identified here included BRAF+, BRCA1-, NOTCH1-, HOXA9- and ERG+ and has been studied by different authors in different cell lines of which four were of human and one of mouse origin (Table 2). Moreover, three different kinds of microarray chips were used for the measurements. Therefore, the similarity observed is likely not based on experimental variations but rather reflects relevant changes in gene expression and commonalities following perturbations of the above-noted cancer genes. We note that there were 10866 genes common to all five experiments. Genes with average ratios below the mean of up-regulated genes or above

**Table 2.** GEO Series in the most significant group of five experiments from clustering.

Target	Type	Author	Cells	GSE	Array	N
BRAF	OE	Ryu	Melanocyte	13827	A1	17256
BRCA1	KD	Lee	MCF10A	4750	A1	17256
HOXA9	KD	Faber	Leukemia	13714	A2	12186
ERG	OE	Carver	HEK-293	14595	A2	12186
NOTCH1	KO	Kopan	Hair follicle	6867	A3	15125

Abbreviations: GSE, GEO Series identifier; N, number of probes mapped to human genes; Experiment types: OE, Over-expression; KD, Knock-down; KO, Knock-out; Array names: A1, Affymetrix Human Genome U133 Plus 2.0; A2, Affymetrix Human Genome U133A 2.0; A3, Affymetrix Mouse Genome 430 2.0.

the mean of down-regulated genes were excluded to obtain a set of 1296 regulated genes.

Table 3 lists the 20 genes exhibiting comparably small standard deviation along with their function and ratios from each of the five measurements. Most of these genes control growth directly or through signaling events. The three genes most highly up-regulated were previously shown to contribute to tumor development and include ubiquitin specific peptidase 2 (USP2),¹⁴ duffy blood group chemokine receptor (DARC)¹⁵ and C-C motif chemokine receptor 3 (CCR3).¹⁶ The EED gene is a member of the Polycomb-group (PcG) family, which form multimeric protein complexes involved in maintaining the transcriptional repressive

state of genes. The down-regulation of the EED gene on activation of the oncogene BRAF as well as on inactivation of the tumor suppressor BRCA1 leads to inactivation of gene silencing, pointing to a possible mechanism of neoplastic transformation mediated by these distinct cancer genes.

The Oncomine database¹⁷ was used to check for consistent differential expression in actual cancer tissue. Table 3 contains the number significant unique analyses showing up- or down-regulation in the 10% rank percentile, *P*-value below 1e-4 and fold-change above 2.0.

From this list, five genes (IDI1, CHST1, ADNP2, EED, EDNRA) showed consistent differential

Table 3. Top 20 most similar regulated genes in the group of five experiments.

Gene	StdDev	Function	bra	brc	hox	ERG	not	C+	C-
DDX50	0.048	RNA helicase	-0.15	-0.27	-0.15	-0.18	-0.14	1	1
USP2	0.058	Peptidase	0.27	0.38	0.22	0.35	0.29	1	26
NCAPD2	0.059	Protein binding	-0.22	-0.22	-0.14	-0.09	-0.08	21	3
DARC	0.067	Cytokine binding	0.18	0.27	0.15	0.33	0.21	4	46
CCR3	0.069	Cytokine binding	0.4	0.49	0.38	0.33	0.51	0	0
NUP37	0.07	Nuclear pore	-0.25	-0.14	-0.07	-0.21	-0.08	17	1
PSMG1	0.071	Chaperone	-0.2	-0.07	-0.19	-0.22	-0.04	17	6
IDI1	0.072	Isomerase	-0.16	-0.18	-0.19	-0.21	-0.01	1	6
LRIT1	0.072	Protein binding	0.22	0.17	0.29	0.39	0.28	0	1
NOL4	0.075	DNA binding	0.28	0.38	0.31	0.46	0.25	5	10
RPA2	0.075	DNA replication	-0.28	-0.12	-0.15	-0.06	-0.11	2	1
CHST1	0.076	Transferase	0.31	0.29	0.12	0.21	0.14	5	3
PCBP1	0.078	Translation regulator	-0.2	-0.1	-0.18	-0.25	-0.03	2	2
HAT1	0.079	Transferase	-0.17	-0.04	-0.18	-0.26	-0.07	18	1
ADNP2	0.079	Transcription regulator	-0.28	-0.1	-0.15	-0.04	-0.18	3	1
CD7	0.079	Receptor	0.29	0.19	0.14	0.36	0.28	2	8
DEK	0.08	Transcription regulator	-0.23	-0.08	-0.08	-0.25	-0.07	17	3
EED	0.081	Transferase	-0.26	-0.16	-0.2	-0.15	-0.02	1	2
KDR	0.081	Growth factor receptor	0.25	0.34	0.2	0.39	0.17	1	11
EDNRA	0.081	Peptide receptor	0.23	0.22	0.18	0.33	0.08	31	17

Notes: Values are log10 ratios between induced and control. C+/C-: number significant unique analyses of cancer tissue in the Oncomine database showing up/down-regulation in the 10% rank percentile, *P*-value below 1e-4 and fold-change above 2.0.

Abbreviations: StdDev, standard deviation; bra, BRAF+; brc, BRCA1-; hox, HOXA9-; ERG, ERG+; not, NOTCH1-.



expression in a majority of analyses represented in Oncomine (see Table 3). Thirteen genes (DDX50, USP2, NCAPD2, DARC, NUP37, PSMG1, NOL4, RPA2, PCBP1, HAT1, CD7, DEK, KDR) showed consistent differential expression in a minority of analyses. Only one gene (LRIT1) was inconsistent and one gene (CCR) did not show differential expression at all.

Checking for over-representation of transcription factors in the TRANSFAC database, we found that with the exception of three genes (CD7, DARC, EDNRA), all genes can be potentially regulated by the transcription factor NF-YA (P -value = $6.79e-04$). NF-YA functions as part of a heterotrimeric complex that activates a number of genes involved in cell cycle regulation, cell proliferation and survival.^{18,19}

Networks

The expression value matrix for the analyzed cancer genes contained 9% missing values, as they were present in essentially all arrays used as a basis for this study. Inspection of the network of protein interactions (Fig. 2) showed that Mitogen-activated protein kinase 1 (MAP2K1), Notch homolog 1 (NOTCH1), V-myc myelocytomatosis viral oncogene

homolog (MYC), and Paired box 5 (PAX5) were the most highly interconnected genes, connecting each to more than six other nodes. This observation was constant at all combination of thresholds. For MYC and MAP2K1, PubMed articles confirmed many of the interactions, but only one was found for NOTCH1 and PAX5. This indicates novel links to PAX5 and NOTCH1, outlining a previous unrecognized importance for these potential cancer genes.

The expression value matrix was randomized and the resulting network compared to the one created from experimental data. In the randomized data network, node connectivity was decreased to 2.2 from 3.8 in experimental data. The number of predicted connections confirmed by publications in PubMed dropped from 16 in experimental to 4 in randomized data.

Looking at sub-networks revealed verifiable sequences of interactions between genes, as shown in Figure 3. This sub-network contained retinoblastoma 1 (RB1) (+), homeobox A9 (HOXA9) (-), Phosphatase and tensin homolog (PTEN) (-), PAX5 (-), and Transferrin receptor (TFRC) (-). These results therefore predict that RB1, a key regulator of entry into cell division, can be connected to TFRC, which

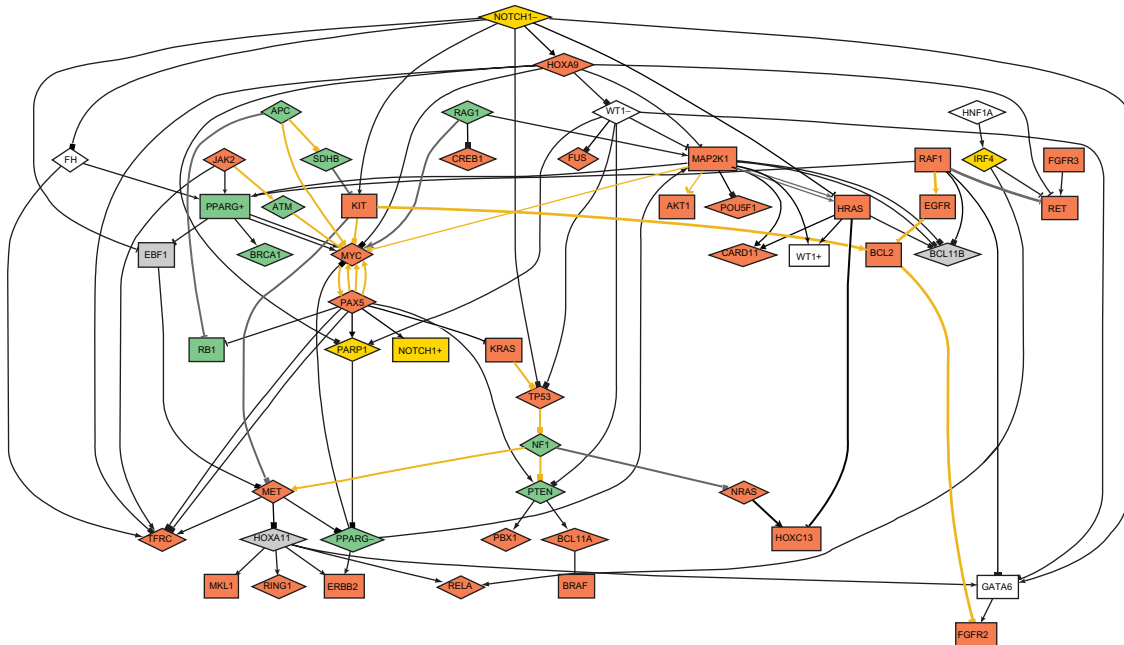


Figure 2. Logical network at P -value below 0.01 and $\text{abs}[\log(\text{ratio})]$ above 1.5.

Notes: Rectangle: increased expression; Diamond: decreased expression; Pointy arrow: up-regulation; Curved: up-regulation linked to up-expression; Tee: down-regulation; Block: down-regulation linked to down-expression; Golden edges: confirmed by PubMed evidence; Gray: false positive evidence; Black: no evidence; red node background: tumor promoting gene; green node background: tumor suppressive gene; yellow node background: tumor promoting and suppressive gene.

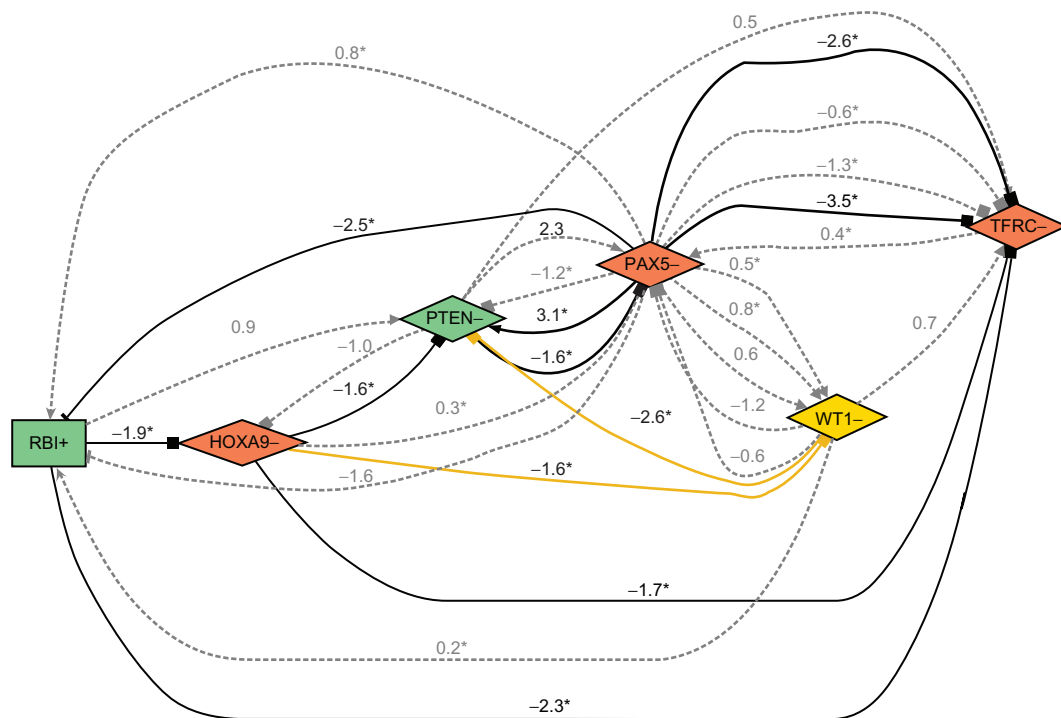


Figure 3. Sub-network of the above network.

Notes: Number beside edge: gene expression change in target gene as log(ratio). The asterisk symbol (*) marks significant changes resulting in *t*-test *P*-values below the threshold of 0.01.

regulates cellular uptake of iron, an element known to be required for cell division. This is confirmed by the measurement of a down-regulation of TFRC in the RB1 up-regulation experiment and can therefore serve as an internal validation of the prediction.

Conclusions

Through analysis of a large set of gene expression data publicly available, we were able to identify a select class of cancer-causing genes whose activities converge to deregulate a common transcription program. This finding is surprising, as the products of the identified cancer-causing genes are known to function in distinct signaling pathways. However, tumor cell evolution proceeds via a process in which genetic changes confer one or another type of growth advantage. Therefore, it is conceivable that changes in the gene expression signature described here mediate a specific aspect of tumor cell evolution. Clearly, the methodology reported here allows to extract from the inundation of gene expression information key patterns of gene expression and to connect them to the deregulation of specific cancer-causing gene products.

Author Contributions

NF, IC and WK conceived the study. NF wrote the programs for the methodology. IC and PW annotated the cancer studies. NF and WK principally wrote the paper, with revisions and contributions from IC. All authors read and approved the final manuscript.

Acknowledgments

We thank Dr. Rehrauer (FGCZ, Zurich) and Dr. Joachim Buhmann (Laboratory of Machine Learning, ETH Zurich) for helpful comments on the manuscript.

Funding

This work was supported in part by the Competence Center for Systems Physiology and Metabolic Disease.

Disclosures and Ethics

As a requirement of publication author(s) have provided to the publisher signed confirmation of compliance with legal and ethical obligations including but not limited to the following: authorship and contributorship, conflicts of interest, privacy and confidentiality and (where applicable) protection of human and



animal research subjects. The authors have read and confirmed their agreement with the ICMJE authorship and conflict of interest criteria. The authors have also confirmed that this article is unique and not under consideration or published in any other publication, and that they have permission from rights holders to reproduce any copyrighted material. Any disclosures are made in this section. The external blind peer reviewers report no conflicts of interest.

References

1. Kulesh DA, Clive DR, Zarlenga DS, Greene JJ. Identification of interferon-modulated proliferation-related cDNA sequences. *Proc Natl Acad Sci U S A*. 1987;84:8453–7.
2. Barrett T, Troup DB, Wilhite SE, et al. NCBI GEO: archive for high-throughput functional genomic data. *Nucleic Acids Res*. 2009;37:D885–90.
3. Brazma A, Hingamp P, Quackenbush J, et al. Minimum information about a microarray experiment (MIAME)—toward standards for microarray data. *Nat Genet*. 2001;29:365–71.
4. Futreal PA, Coin L, Marshall M, et al. A census of human cancer genes. *Nat Rev Cancer*. 2004;4:177–83.
5. Rhodes D, Chinnaiyan A. Integrative analysis of the cancer transcriptome. *Nat Genet*. 2005;37:S31–7.
6. Ramaswamy S, Ross KN, Lander ES, Golub TR. A molecular signature of metastasis in primary solid tumors. *Nat Genet*. 2003;33:49–54.
7. Creighton CJ. Multiple oncogenic pathway signatures show coordinate expression patterns in human prostate tumors. *PloS One*. 2008;3:1–8.
8. Sayers EW, Barrett T, Benson DA, et al. Database resources of the National Center for Biotechnology Information. *Nucleic Acids Res*. 2009;37:5–15.
9. R Development Core Team. *R: A Language and Environment for Statistical Computing*. R Foundation for Statistical Computing, Vienna, Austria. ISBN 3-900051-07-0. 2008.
10. Suzuki R, Shimodaira H. Pvcust: an R package for assessing the uncertainty in hierarchical clustering. *Bioinformatics*. 2006;22:1540–2.
11. Ellson J, Gansner E, Koutsofios E, North S, Woodhull G. Graphviz and dynagraph—static and dynamic graph drawing tools. In: Junger M, Mutzel P, editors. *Graph Drawing Software*. 2003:127–48. Springer-Verlag.
12. Pietriga, E. A toolkit for addressing hci issues in visual language environments. *IEEE Symposium on Visual Languages and Human-Centric Computing (VL/HCC '05)*. Dallas, TX, USA. September 2005:145–52.
13. Matys V, Fricke E, Geffers R, et al. TRANSFAC: transcriptional regulation, from patterns to profiles. *Nucleic Acids Res*. 2003;31:374–8.
14. Priolo C, Tang D, Brahamandan M, et al. The isopeptidase USP2a protects human prostate cancer from apoptosis. *Cancer Res*. 2006;66:8625–32.
15. Lentsch AB. The Duffy antigen/receptor for chemokines (DARC) and prostate cancer. A role as clear as black and white? *FASEB J*. 2002;16:1093–5.
16. Jaehrer K, Zelle-Rieser C, Perathoner A, et al. Up-regulation of functional chemokine receptor CCR3 in human renal cell carcinoma. *Clin Cancer Res*. 2005;11:2459–65.
17. Rhodes DR, Yu J, Shanker K, et al. ONCOMINE: a cancer microarray database and integrated data-mining platform. *Neoplasia*. 2004;6:1–6.
18. Bhattacharya A, Deng JM, Zhang Z, Behringer R, de Crombrughe B, Maity SN. The B subunit of the CCAAT box binding transcription factor complex (CBF/NF-Y) is essential for early mouse development and cell proliferation. *Cancer Res*. 2003;63:8167–72.
19. Caretti G, Salsi V, Vecchi C, Imbriano C, Mantovani R. Dynamic recruitment of NF-Y and histone acetyltransferases on cell-cycle promoters. *J Biol Chem*. 2003;278:30435–40.